جامعة الملك عبدالله
للعلوم والتقنية
King Abdullah University of
Science and Technology

High-Performance 1.55-μm Superluminescent Diode Based on Broad Gain InAs/InGaAlAs/InP Quantum Dash Active Region

Item Type	Article
Authors	Khan, Mohammed Zahed Mustafa;Ng, Tien Khee;Ooi, Boon S.
Citation	High-Performance 1.55-μm Superluminescent Diode Based on Broad Gain InAs/InGaAlAs/InP Quantum Dash Active Region 2014, 6 (4):1 IEEE Photonics Journal
Eprint version	Publisher's Version/PDF
DOI	10.1109/JPHOT.2014.2337892
Publisher	Institute of Electrical and Electronics Engineers (IEEE)
Journal	IEEE Photonics Journal
Rights	(c) 2014 IEEE. Personal use of this material is permitted. Permission from IEEE must be obtained for all other users, including reprinting/ republishing this material for advertising or promotional purposes, creating new collective works for resale or redistribution to servers or lists, or reuse of any copyrighted components of this work in other works.
Download date	2023-12-06 21:39:34
Link to Item	http://hdl.handle.net/10754/528238

IEEE Photonics Journal
An IEEE Photonics Society Publication

Open Access

High-Performance 1.55-μm Superluminescent Diode Based on Broad Gain InAs/InGaAlAs/InP Quantum Dash Active Region

Volume 6, Number 4, August 2014

M. Z. M. Khan, Member, IEEE
T. K. Ng, Member, IEEE
B. S. Ooi, Senior Member, IEEE

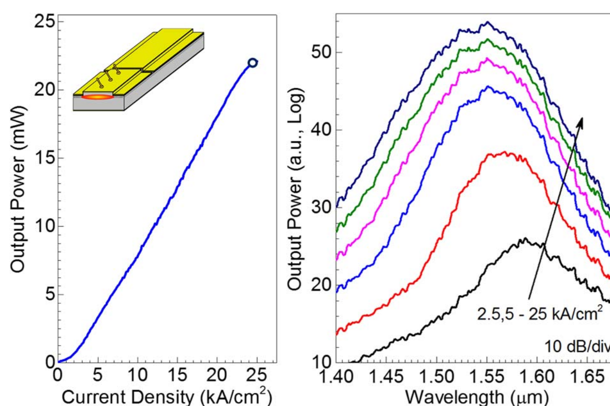

DOI: 10.1109/JPHOT.2014.2337892
1943-0655 © 2014 IEEE

IEEE photonics SOCIETY

IEEE

High-Performance 1.55-μm Superluminescent Diode Based on Broad Gain InAs/InGaAlAs/InP Quantum Dash Active Region

M. Z. M. Khan, *Member, IEEE*, T. K. Ng, *Member, IEEE*, and B. S. Ooi, *Senior Member, IEEE*

Photonics Laboratory, Computer, Electrical, and Mathematical Science and Engineering Division, King Abdullah University of Science and Technology (KAUST), Thuwal 23955-6900, Saudi Arabia

DOI: 10.1109/JPHOT.2014.2337892
1943-0655 © 2014 IEEE. Translations and content mining are permitted for academic research only. Personal use is also permitted, but republication/redistribution requires IEEE permission. See http://www.ieee.org/publications_standards/publications/rights/index.html for more information.

Manuscript received May 14, 2014; revised July 1, 2014; accepted July 1, 2014. Date of publication July 10, 2014; date of current version August 5, 2014. This work was supported by King Abdullah University of Science and Technology's Competitive Research Grant CRG-1-2012-OOI-010. Corresponding author: B. S. Ooi (e-mail: boon.ooi@kaust.edu.sa).

Abstract: We report on the high-performance characteristics from superluminescent diodes (SLDs) based on four-stack InAs/InGaAlAs chirped-barrier thickness quantum dash (Qdash) in a well structure. The active region exhibits a measured broad gain spectrum of $\sim$140 nm, with a peak modal gain of $\sim$41 cm^{-1}. The noncoated two-section gain-absorber broad-area and ridge-waveguide device configuration exhibits an output power of $>$ 20 mW and $>$ 12 mW, respectively. The corresponding $-$3-dB bandwidths span $\sim$82 nm and $\sim$72 nm, with a small spectral ripple of $<$ 0.2 dB, related largely to the contribution from dispersive height dash ensembles of the highly inhomogeneous active region. These C-L communication band devices will find applications in various cross-disciplinary fields of optical metrology, optical coherent tomography, etc.

Index Terms: Quantum dash, superluminescent diode, broad gain, chirp design, inhomogeneous broadening, C-L band devices.

1. Introduction

Superluminescent diodes (SLDs or SLEDs) has diverse applications viz. metrology, spectroscopy and sensing, imaging, apart from their telecom applications such as tunable source, short pulse generation, broadband light sources in wavelength division multiplexed systems, etc. [1], [2]. The matured GaAs material system was the favorite contender for realizing these devices because of their wavelength span near 1.31 μm offering lowest dispersion. Moreover, in the field of biological imaging, GaAs based SLD are already established sources for the optical coherent tomography (OCT) applications. Enhancing the power-bandwidth product (PBP) of SLD devices is of prime importance and main technological challenge [3]. Various approaches have been attempted to achieve this target via self-assembled InAs/GaAs quantum dot (Qdot) active region and exploiting their natural inhomogeneous broadening which enhances the gain profile and hence, the spectral width of SLDs. Intentional chirping of the energy levels of the multi-layer Qdots via altering the growth conditions to induce large dot size dispersion [4], hybrid quantum well (Qwell)/Qdot structures [5] or using multi-contact device structures [2], [6] have been

reported. In general, wide-emission bandwidth of ∼100–200 nm with power in few tens of milliwatts has been demonstrated. Recently, an emerging technique based on post-growth bandgap engineering has also shown to improve the SLD characteristics. Ultra-broad emission in the range of ∼200–300 nm are realized from InAs/GaAs Qdot SLDs utilizing rapid thermal annealing, modulation p-doped multi-section device intermixing [1], and selective area intermixing [7]. In general, these demonstrations highlight the potential of self-assembled growth technology in realizing broadband semiconductor devices.

Broadband devices spanning S-C-L communication bands has also found attention because of their broader cross-disciplinary field applications in optical metrology [8]–[10] (gyroscopes, optical time domain reflectometery), and particularly, in monitoring environmental health via managing emission of green house gases and hazardous chemicals sensing [8], for instance, CO, CO_2, NH_3, CH_4, etc., which have their absorption peak within this window, besides telecom applications (wavelength division multiplexed system) [1], [11], [12]. Although the S-C-L wavelength window includes the primary water absorption peaks, the attractive feature of greater penetration depth offered by ∼1.5–1.6 μm SLDs makes them a potential candidate in dentistry and bone-related disease OCT imaging [13]–[16]. Furthermore, 1.55 μm OCT systems has also attracted in non-biomedical field applications such as non-destructive testing, dimensional metrology, etc. [17]. 1.5 μm SLD devices based on InGaAsP/InP multiple quantum well (Qwell) active region has dominated this wavelength window for more than two decades [9], [10]. On this very matured active region material system, as grown [18] and selective area grown [8] SLDs has been reported with output power (bandwidth) ∼20 mW (∼130 nm) and ∼100 mW (∼61 nm) with low spectral ripple. In fact, the commercially available SLD devices, to the best of our knowledge, are also based on this material system, with fiber coupled output power (bandwidth) ranging from ∼40 mW (∼33 nm) to ∼10 mW (∼100 nm) [19]–[21]. In general, the PBP achieved in this material system is ∼1000–2600 mWnm. However, the thrust to enhance the efficiency and achieve comparatively flat emission bandwidth, which is rather limited in Qwell active region, lead to the exploration of new material system in the form of self assembled InAs Qdashes on InP platform which has mixed features of Qdots and Qwells, and spanning ground state (GS) emission around ∼1.4–2.0 μm. With this hardly a decade old material platform, we were the first to demonstrate a wideband emission from InAs/InP Qdash SLDs spanning ∼110 nm and output power ∼1.5 mW utilizing the natural inhomogeneity of the Qdash active region [12].

Here, we report on the implementation of chirped multi-stack dash-in-a-well active region device platform in achieving broad gain and high performance characteristics in the amplified spontaneous emission (ASE) via SLD investigation. The highly dispersed active region optical transition is achieved by varying the InGaAlAs barrier layer thickness in the multi-stack device structure. A broad gain bandwidth of ∼140 nm is measured from this active region material, and when implemented as a broad area (ridge-waveguide) SLD device, an output power > 20 mW (> 12 mW) and emission bandwidth ∼82 nm (∼72 nm) is achieved. This is a significant increase (> 8 times) in the PBP value (∼1800 mWnm) when compared to the reported SLDs on an identical active region material platform (∼165 mWnm) [12] and similar PBP value when compared to the matured InGaAsP/InP Qwell platform [19]–[21].

2. Experimental Details

The chirped InAs Qdash device structure was grown by molecular beam epitaxy (MBE) on n-InP (001) substrate. The active region comprises of four stacks of 5 ML InAs Qdash in a 7.6 nm thick compressively strained $In_{0.64}Ga_{0.16}Al_{0.2}As$ asymmetric quantum well, separated by different barrier thickness [20, 15, 10, 10 nm (top)] $In_{0.5}Ga_{0.32}Al_{0.18}As$ tensile strained layers starting from a 25 nm bottom layer. The active region is sandwiched between 250 nm lattice matched $In_{0.52}Ga_{0.28}Al_{0.2}As$ separate confinement heterostructure layer and then by $In_{0.25}Al_{0.48}As$ waveguide claddings. A partial schematic diagram of the device structure is shown in Fig. 1(a) and more details can be found elsewhere [22]. The SLD design is based on two isolated sections; gain and absorber region. While the gain region is pumped, the absorber section is left

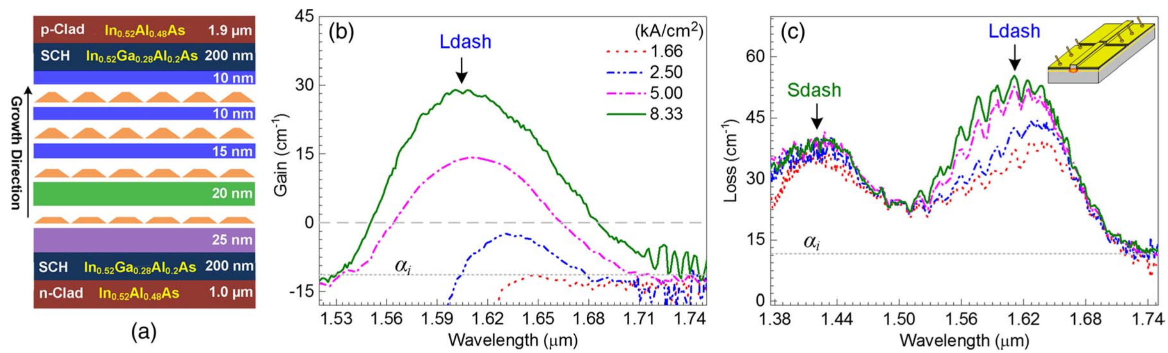

Fig. 1. (a) Schematic description of the device waveguide structure, measured (b) gain [modal gain $-\alpha_i$] and (c) absorption [modal absorption $+\alpha_i$] spectra at different current density, obtained from 3×1000 μm^2 multi-section device, in CW mode. Blue, green, and violet colors in (a) are $In_{0.5}Ga_{0.32}Al_{0.18}As$ barrier layers with embedded white $In_{0.64}Ga_{0.16}Al_{0.2}As$ Qwell and orange pyramidal InAs Qdashes. The spectral modulation in (b) and (c) are due to the external cavity formation between the device and the butt coupled multi-mode fiber facet.

un-pumped as it acts as a photon absorber, thus suppressing the optical feedback from the rear as cleaved facet and minimizing the lasing action. The SLDs are fabricated using standard broad area/ridge-waveguide laser fabrication process including an extra isolation step to separate the gain and absorber sections. In addition, multi-section ridge-waveguide devices were also fabricated with each section length 3×1000 μm^2, for absorption/gain measurement of the chirped Qdash material following technique described in [23]. The broad area 20×1000 μm^2 and ridge-waveguide 4×2500 μm^2 SLD devices with as-cleaved facet and $\sim$1000 μm absorber section were tested under short pulsed (SP) mode at 0.5 μs current pulse width and 0.2% duty cycle while the gain/absorption measurements were carried out under continuous-wave (CW) operation. In addition, to show the quality of the chirped Qdash material, broad area 20×1000 μm^2 and ridge-waveguide 4×2500 μm^2 lasers are also fabricated from the same wafer and tested under SP mode operation. For spectral analysis, the optical power is butt-coupled into a standard multi-mode fiber. Spectral modulations are observed in all the emission spectra, with relatively fixed modulation period, owing to the external cavity formation between the device and the bare-fiber facets.

3. Material Characterization

Utilizing the segment contact method, the optical gain and absorption spectra of the chirped Qdash active region is calculated and plotted in Fig. 1(b) and (c), respectively, and at four different current injections. A very broad gain and absorption profile is observed from this class of active region material indicating a highly inhomogeneous Qdash system, a direct effect of intentionally enhanced GS optical transitions via varying the barrier thickness. The extracted internal loss from both the spectra is $\alpha_i \sim 12 \pm 2$ cm^{-1} while the transparency current density is estimated to be $J_{tr} \sim 2.5$ kA/cm^2 from Fig. 1(b). A single peak gain bandwidth of $\sim$140 nm is achieved at a current density of 8.33 kA/cm^2 with peak modal gain $\sim$41 cm^{-1}. On the other hand two peaks are observed in the absorption spectra as depicted in Fig. 1(c) centered at $\sim$1.42 μm and $\sim$1.61 μm. We attribute the long wavelength absorption peak to the filling of carriers first by large average height dash ensembles (Ldash) corresponding to the 10 nm and 15 nm barrier thickness Qdash layers. We postulate that these Qdash stacks contribute collectively in the ASE regime under the CW operation because of comparatively small barrier thickness which assists carrier tunneling [22]. The short wavelength absorption peak is attributed to the short average height dash (Sdash) ensembles corresponding to the 20 nm barrier thickness dash layer. These attributions are further supported by our recent systematic investigation via photoluminescence measurements and a statistical dash height analysis using transmission

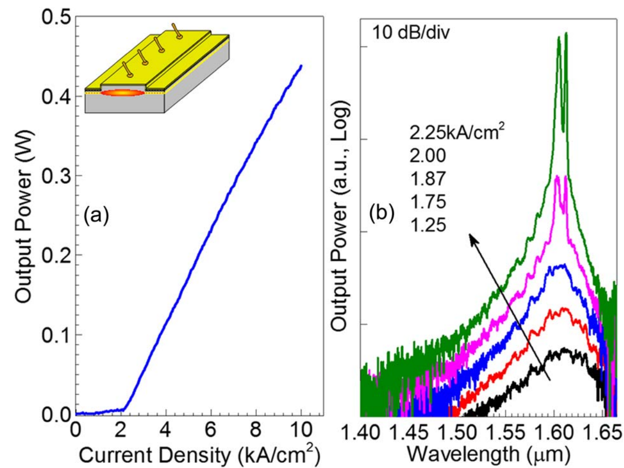

Fig. 2. Room temperature L-I characteristics of as-cleaved 20×1000 μm^2 broad area Qdash laser in SP mode operation. The corresponding measured lasing spectra around the threshold current density $J_{th} \sim 2.0$ kA/cm^2.

electron microscopy on this chirped Qdash active region material. The results revealed large (small) average dash height from the 10 (20) nm Qdash stack resulting in smaller (larger) optical transitions. The peak loss value of the Ldash ensemble is far larger than the Sdash ensemble ($>$ by 13 cm^{-1}) suggesting that their gain is limited. This could partly be attributed to the photon re-absorption process in the system i.e., Sdashes (emitting high energy photons) acts as carrier feeders to the Ldash assembly (small average band transition energy) via optical pumping. This might be the reason that only single lobe gain profile owing to Ldash assembly is observed. Furthermore, this can also be attributed to the non-uniform distribution of the carriers in the Qdash layers with more carriers filling up the dashes near to p-cladding side (i.e., Ldash group) than the n-cladding side; probably a result of lower hole mobility in the barriers separating the layers, as observed in the Qwell devices [24]. In general, such a broad gain profile material with high peak gain value is very attractive as broadband semiconductor optical amplifier (SOA), modulator, sources, and detectors in the telecom window.

Fig. 2 illustrates the room temperature L-I characteristics of 20×1000 μm^2 broad area chirped Qdash laser under SP mode operation. A high total output power of $>$ 0.4 W is measured, as shown in Fig. 2(a) without any sign of optical power roll off. The electroluminescence of the device below and above threshold current density ($J_{th} \sim 2.0$ kA/cm^2) is plotted in Fig. 2(b). A broad spontaneous emission spectra is observed with subsequent lasing at $\sim$1.61 μm, on increasing injection current density from 1.25 kA/cm^2 to 2.25 kA/cm^2. The internal quantum efficiency η_i, α_i, and J_{tr} are extracted from the laser cavity length dependence of external differential quantum efficiency and the threshold current density. The corresponding values are $\sim$70%, $\sim$11 cm^{-1}, and $\sim$1.6 kA/cm^2, respectively. A small discrepancy in α_i, and J_{tr} is observed on comparing with the extracted values obtained from the gain/absorption measurements owing to the different mode of current pumping in both cases (CW mode versus SP mode operation) since the chirped Qdash lasers show strong dependence of J_{th} with operating temperature due to a lower value of characteristic temperature, $T_0 \sim 60$ K [25]. Therefore, increased non-radiative recombination and thermionic emission is expected in the CW mode compared to the pulsed mode operation.

4. SLD Characterization

Fig. 3(a) shows the L-I characteristics of 20×1000 μm^2 broad area chirped Qdash SLD device, operated under SP mode and at room temperature. The ASE spectra measured at different injection current density is shown in Fig. 3(b). A super-linear optical power behavior is

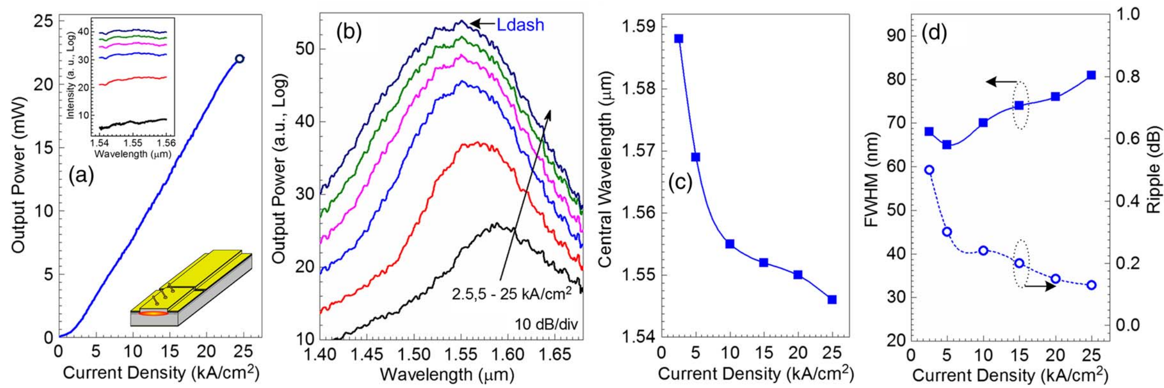

Fig. 3. Room temperature (a) L-I characteristics of 20×1000 μm^2 Qdash broad area SLD in SP mode operation and with an integrated 1000 μm photon absorber section. (b) Wideband emission spectra of the SLD at different injection current density at 2.5 kA/cm^2 and 5–25 kA/cm^2 in steps of 5 kA/cm^2. The corresponding summary of the change in (c) central emission wavelength and (d) emission bandwidth and spectral ripple, as a function of injection current density of the SLD. The inset of (a) shows the spectral ripple within 20 nm range from central emission wavelength at different injections. The emission spectra in (b) are vertically offset for clarity. The solid and dashed lines in (c) and (d) are a guide for the eyes.

evident with increasing current injection. A maximum output power of $>$ 20 mW is measured at 25 kA/cm^2 without apparent power roll-off. At this current injection, the emission bandwidth as large as $\sim$82 nm is achieved, centered at $\sim$1.55 μm (calculated by identifying the central wavelength at full-width-at-half-maximum), and resulting in a PBP $\sim$1800 mWnm. The broadening and blue shifting of the emission wavelength versus the injection current is summarized in Fig. 3(c) and (d). The central emission wavelength ($\sim$1.59 μm) of the SLD and the lasing wavelength ($\sim$1.61 μm) of the laser diode at $<$ 2.5 kA/cm^2 are comparable signifying the quenching of the lasing action and transition from the spontaneous emission to the ASE regime. A large wavelength blue shift of $\sim$21 meV and an increase in the emission bandwidth by $\sim$12 nm is observed on increasing the current density from 2.5 to 25 kA/cm^2, thus providing an estimate of the degree of active region inhomogeneity. In general, the emission is dominated by smaller height dashes (emitting at shorter wavelength) due to larger photon re-absorption by the larger height dashes (emitting at larger wavelength) of the Ldash assembly. Once the rate of photon generation by shorter dashes exceeds the photon absorption by larger dashes, the intensity related to these quantized states starts to increase and hence blue shifts the emission spectra. With increasing injection, the simultaneous and comparable emission from both shorter and larger dashes of Ldash ensemble results in broadening of the emission bandwidth. From Fig. 3(d), the residual Fabry–Perot oscillations of $<$ 0.2 dB is observed for injection current densities $>$ 5 kA/cm^2. This extremely small spectral ripples over the 10 nm span from the central emission wavelength is comparable to the different SLD device configurations on InAs/GaAs Qdot and InGaAsP/InP Qwell material system [1], [18]. This high performance characteristic with large PBP and low spectral ripple from the chirped Qdash SLD affirms the potential of this device structure platform for further advancing and realizing ultra-broadband semiconductor emitters. The device theoretical coherence length in air $L_c \approx 0.8825\lambda^2/\Delta\lambda$ is $\sim$ 25.7 μm, where λ is the central wavelength and $\Delta\lambda$ is the emission bandwidth; and the average spectral power density (optical power/bandwidth) is $\sim$0.22 mW/nm. The simultaneous achievements of low L_c and high PBP, which is rather difficult, makes the device highly attractive S-C-L broadband source for OCT applications. It is noteworthy to mention that the power values could further be increased by different techniques such as facet coatings, utilizing longer tapered and multi-section devices [4], SOA in tandem with the SLD devices [6].

Next, we characterize a ridge-waveguide Qdash SLD device, fabricated from the same chirped Qdash active region epitaxial wafer. The results are shown in Fig. 4 for a 4×2500 μm^2

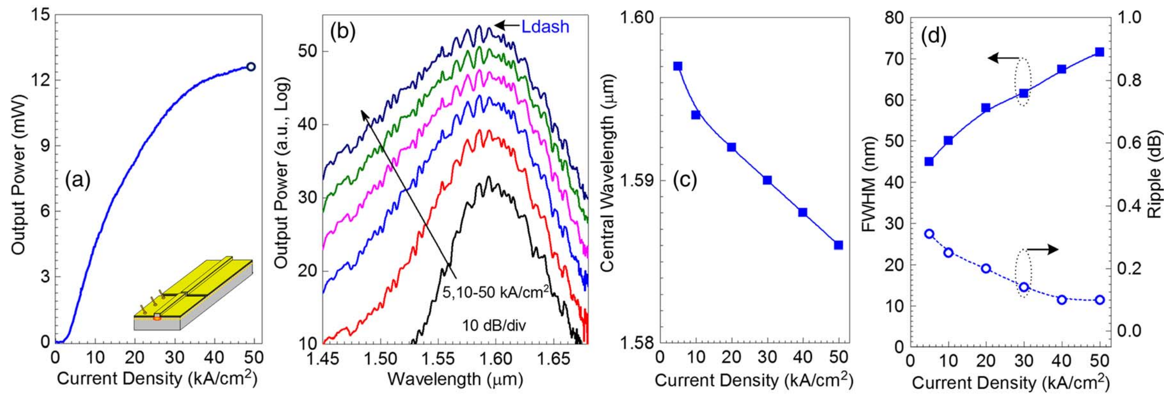

Fig. 4. Room temperature (a) L-I characteristics of $4 \times 2500\ \mu m^2$ Qdash ridge-waveguide SLD in SP mode operation and with an integrated 1000 μm photon absorber section. (b) Wideband emission spectra of the SLD at different injection current density at 5 kA/cm^2 and 10–50 kA/cm^2 in steps of 10 kA/cm^2. The corresponding summary of the change in (c) central emission wavelength and (d) emission bandwidth and spectral ripple, as a function of injection current density of the SLD. The emission spectra in (b) are vertically offset for clarity. The solid and dashed lines in (c) and (d) are a guide for the eyes.

device under the SP operation and at room temperature. Similar behavior in the L-I and emission spectra is observed compared to the broad area SLD device. An output power of as large as $>$ 12 mW is measured at 50 kA/cm^2 with large emission bandwidth ($\sim$72 nm), centered at $\sim$1.59 μm [see Fig. 4(b)], and attributed to the inhomogeneous optical transitions from Ldash ensemble. A red shift in the central emission wavelength of $>$ 20 nm is observed in this case compared to the broad area SLDs. We partly attribute this observation to the different active region volume of both the devices (10^{-4} cm^2 in this case compared to 2×10^{-4} cm^2 for the broad area SLD). The red shift of $\sim$21 meV with dominant central emission at $\sim$1.59 μm from ridge-waveguide SLD suggests comparatively less photon re-absorption in the Qdash system, possibly due to reduction in the active region volume, which lead to emission from comparatively larger height dashes from the Ldash assembly. Besides, we also partly ascribe the above observation to the different behavior of the Qdash system in both the devices due probably to the alteration in the active region temperature (due to different device geometrical parameters) with increasing current injection which would lead to non-uniform carrier distribution among the inhomogeneous Qdashes via thermionic emission and carrier tunneling processes [22]. A differing observation of small central wavelength blue shift ($\sim$5.4 meV) and large increase in bandwidth ($\sim$27 nm) with current pumping (depicted in Fig. 4(c) and (d), respectively), in the ridge-waveguide SLDs, further supports our attributions. The measured spectral ripple is $<$ 0.3 dB for the entire current injection range and the calculated PBP and the coherence length in air of the device, at the maximum current injection, is $\sim$905 mWnm and $\sim$30.8 μm, respectively.

An extended SP mode emission spectrum of the ridge-waveguide SLD at three different current injections is plotted in Fig. 5(a) which shows an interesting feature [26]. Two additional emission humps at $\sim$1.4 μm and $\sim$1.2 μm is visible which is ascribed to the emission from Sdash ensemble and the Qwells, respectively. An energy band model sketch describing the behavior of the active region is also shown in the inset of Fig. 5(c). Although a collective contribution of Sdash and Ldash ensembles forms an overall SLD emission signature with very wide coverage of $\sim$400 nm at high injections, an emission intensity difference of $>$ 30 dB between Sdash and Ldash groups shadowed the Sdash existence. However, in the case of CW operation of the ridge-waveguide SLD, depicted in Fig. 5(b) and (c), a comparable simultaneous emission from all the quantum confined nanostructures at high injections lead to the realization of an extra-ordinary emission bandwidth from our chirped SLD devices. A CW output power of $\sim$1.3 mW with an emission bandwidth of $>$ 500 nm is achieved at high current pumping of $>$ 10 kA/cm^2, thanks to the highly inhomogeneous dash-in-well active region together with the

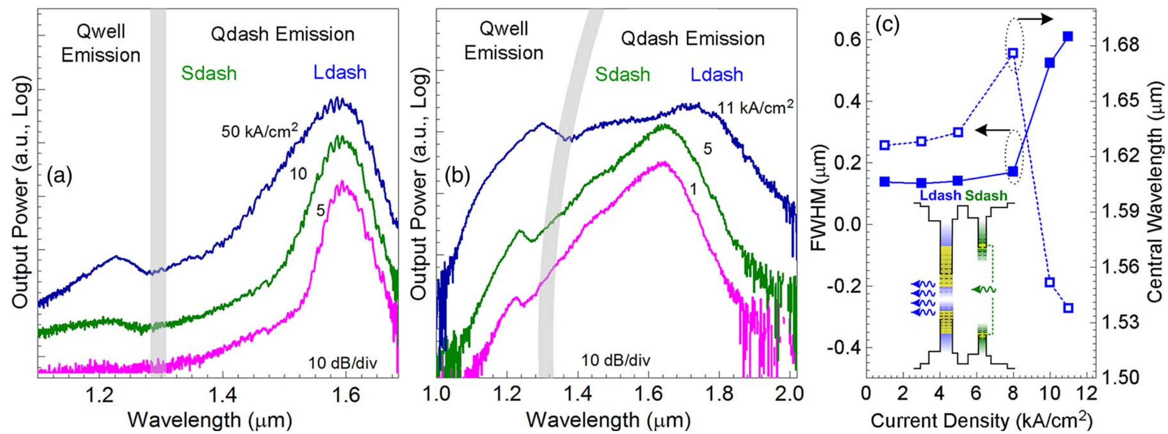

Fig. 5. Extended emission spectra of the 4×2500 μm^2 Qdash ridge-waveguide SLD under (a) SP mode and (b) CW mode operation. (c) Change in central emission wavelength and bandwidth as a function of injection current density of the 4×2500 μm^2 SLD under CW mode operation. The inset of (c) sketches the chirped Qdash active region energy band model showing Ldash and Sdash ensemble and the dominant emission from Ldash group. The emission spectra in (a) and (b) are vertically offset by 5 dB for clarity except the 11 kA/cm^2 spectra, which is offset by 10 dB. The gray shaded region in (a) and (b) qualitatively separates the Qwell and Qdash emission regions, and the solid and dashed lines in (c) are a guide for the eyes.

thermal effects [26]. Comparable emissions from Qdash ensembles and Qwells suggest overcoming the photon-reabsorption process (carrier feeding via optical pumping) in the system which is possible at high current injections. The red shift of Qdash groups and Qwells emission [shown as bending of the respective spectral regions by a gray band in Fig. 5(b)] is indicative of simultaneous emission from shorter transition energy dashes of both the dash ensembles, and different asymmetric Qwells. In addition, the observation is partially attributed to junction heating which also affect the localized distribution of carriers within the dash stack and among the stacks, probably due to thermionic carrier escape [26]. At smaller CW injections, however, the emission is still dominated by only Ldash group, similar to the SP mode operation, with emission bandwidth and output power reaching values $\sim$170 nm and $\sim$1.1 mW, respectively, at 8 kA/cm^2. The observation of simultaneous radiative recombination from Ldash and Sdash groups in SP mode and demonstration of collective emission from Qdash-well under CW operation shows the potential of this active region design platform. Through proper optimization of the device structure by possibly including two 20 nm barrier thickness dash stacks (to increase the Sdash gain) and optimized Qwell heights, the gain bandwidth and hence emission bandwidth of chirped Qdash SLD can be improved substantially.

5. Conclusion

We demonstrated the feasibility of chirped InAs/InP Qdash active region material platform as a viable platform for realizing wide optical bandwidth and high output power light emitting devices. Through the gain-absorber SLD configuration, we achieved a -3 dB bandwidth of $\sim$82 nm and $\sim$72 nm from the broad area and ridge-waveguide devices centered at 1.55 μm. The corresponding measured optical power of $\sim$22 mW and $\sim$12 mW, with low spectral modulation, highlights high performance characteristics from these devices. Further optimization of the Qdash active region would lead to highly efficient and large PBP SLD devices.

References

[1] Z. Y. Zhang, R. A. Hogg, X. Q. Lv, and Z. G. Wang, "Self-assembled quantum-dot superluminescent light-emitting diodes," *Adv. Opt. Photon.*, vol. 2, no. 2, pp. 201–228, Jun. 2010.

[2] H. S. Djie *et al.*, "InGaAs/GaAs quantum-dot superluminescent diode for optical sensor and imaging," *IEEE Sensors J.*, vol. 7, no. 2, pp. 251–257, Feb. 2007.

[3] S. Haffouz, P. J. Barrios, R. Normandin, D. Poitras, and Z. Lu, "Ultrawide-bandwidth, superluminescent light-emitting diodes using InAs quantum dots of tuned height," *Opt. Lett.*, vol. 37, no. 6, pp. 1103–1105, Mar. 2012.
[4] M. A. Majid, M. Hugues, S. Vézian, D. T. D. Childs, and R. A. Hogg, "Optimization of quantum dot molecular beam epitaxy for broad spectral bandwidth devices," *IEEE Photon. J.*, vol. 4, no. 6, pp. 2066–2073, Dec. 2012.
[5] S. Chen *et al.*, "Hybrid quantum well/quantum dot structure for broad spectral bandwidth emitters," *IEEE J. Sel. Topics Quantum Electron.*, vol. 19, no. 4, p. 1900209, Jul./Aug. 2013.
[6] X. Li *et al.*, "A high-performance quantum dot superluminescent diode with a two-section structure," *Nanosci. Res. Lett.*, vol. 6, p. 625, Dec. 2011.
[7] K. Zhou *et al.*, "Quantum dot selective area intermixing for broadband light sources," *Opt. Exp.*, vol. 20, no. 24, pp. 26 950–26 957, Nov. 2012.
[8] J. H. Song, K. Kim, Y. A. Leeam, and G. Kim, "High-power broadband superluminescent diode using selective area growth at 1.5-μm wavelength," *IEEE Photon. Technol. Lett.*, vol. 19, no. 19, pp. 1415–1417, Oct. 2007.
[9] O. Mikami, H. Yasaka, and Y. Noguchi, "Broader spectral width InGaAsP stacked active layer superluminescent diodes," *Appl. Phys. Lett.*, vol. 56, no. 11, pp. 987–989, Mar. 1990.
[10] S. Kondo *et al.*, "Very wide spectrum multiquantum well superluminescent diode at 1.5 μm," *Electron. Lett.*, vol. 28, no. 12, pp. 132–133, Jan. 1992.
[11] B. S. Ooi *et al.*, "Quantum dashes on InP substrate for broadband emitter applications," *IEEE J. Sel. Topics Quantum Electron.*, vol. 14, no. 4, pp. 1230–1238, Jul./Aug. 2008.
[12] H. S. Djie, C. E. Dimas, and B. S. Ooi, "Wideband quantum-dash-in-well superluminescent diode at 1.6 μm," *IEEE Photon. Technol. Lett.*, vol. 18, no. 16, pp. 1747–1749, Aug. 2006.
[13] S. Ishida and N. Nishizawa, "Quantitative comparison of contrast and imaging depth of ultrahigh-resolution optical coherence tomography images in 800–1700 nm wavelength region," *Biomed. Opt. Exp.*, vol. 3, no. 2, pp. 282–294, Feb. 2012.
[14] U. Sharma, E. W. Chang, and S. H. Yun, "Long-wavelength optical coherence tomography at 1.7 μm for enhanced imaging depth," *Opt. Exp.*, vol. 16, no. 24, pp. 19 712–19 723, Nov. 2008.
[15] V. Kodach, J. Kalkman, D. J. Faber, and T. G. van Leeuwen, "Quantitative comparison of the OCT imaging depth at 1300 nm and 1600 nm," *Biomed. Opt. Exp.*, vol. 1, no. 1, pp. 176–185, Aug. 2010.
[16] Y.-S. Hsieh *et al.*, "Dental optical coherence tomography," *Sensors*, vol. 13, no. 7, pp. 8928–8949, Jul. 2013.
[17] D. Stifter *et al.*, "Investigation of polymer and polymer/fibre composite materials with optical coherence tomography," *Meas. Sci. Technol.*, vol. 19, no. 7, p. 074011, Jul. 2008.
[18] J. Song *et al.*, "High-power broad-band superluminescent diode with low spectral modulation at 1.5-/spl mu/m wavelength," *IEEE Photon. Technol. Lett.*, vol. 12, no. 7, pp. 783–785, Jul. 2000.
[19] [Online]. Available: http://www.thorlabs.de/thorcat/22400/SLD1550S-A40-SpecSheet.pdf
[20] [Online]. Available: http://www.exalos.com/downloadform.html?partno=EXS210059-01&pdf=/productinfo/datasheet/EXS210059-01.pdf
[21] [Online]. Available: http://www.exalos.com/downloadform.html?partno=EXS210048-02&pdf=/productinfo/datasheet/EXS210048-02.pdf
[22] M. Z. M. Khan, T. K. Ng, C.-S. Lee, P. Bhattacharya, and B. S. Ooi, "Investigation of chirped InAs/InGaAlAs/InP quantum dash lasers as broadband emitters," *IEEE J. Quantum Electron.*, vol. 50, no. 2, pp. 51–60, Feb. 2014.
[23] P. Blood *et al.*, "Characterization of semiconductor laser gain media by the segmented contact method," *IEEE Sel. Topics Quantum Electron.*, vol. 9, no. 5, pp. 1275–1282, Sep./Oct. 2003.
[24] C.-F. Lin, Y.-S. Su, C.-H. Wu, and G. S. Shmavonyan, "Influence of separate confinement heterostructure on emission bandwidth of InGaAsP superluminescent diodes/semiconductor optical amplifiers with nonidentical multiple quantum wells," *IEEE Photon. Technol. Lett.*, vol. 16, no. 6, pp. 1441–1443, Jun. 2004.
[25] M. Z. M. Khan, T. K. Ng, C.-S. Lee, P. Bhattacharya, and B. S. Ooi, "Chirped InAs/InP quantum-dash laser with enhanced broad spectrum of stimulated emission," *Appl. Phys. Lett.*, vol. 102, no. 9, pp. 091102-1–091102-3, Mar. 2013.
[26] M. Z. M. Khan, M. A. Majid, T. K. Ng, D. Cha, and B. S. Ooi, "Simultaneous quantum dash-well emission in a chirped dash-in-well superluminescent diode with spectral bandwidth $>$ 700 nm," *Opt. Lett.*, vol. 38, 19, pp. 3720–3723, Oct. 2013.